

# The effect of sulphuric acid activation on the crystallinity, surface area, porosity, surface acidity, and bleaching power of a bentonite

Hülya Noyan<sup>a</sup>, Müşerref Önal<sup>b</sup>, Yüksel Sarıkaya<sup>b,\*</sup>

<sup>a</sup> Refik Saydam Hygiene Center (RSHC), Sıhhiye, Ankara, Turkey

<sup>b</sup> Ankara University, Faculty of Science, Department of Chemistry, Beşevler, 06100 Ankara, Turkey

Received 6 December 2006; received in revised form 22 March 2007; accepted 26 March 2007

## Abstract

The Hançılı (Keskin, Ankara, Turkey) bentonite was activated with H<sub>2</sub>SO<sub>4</sub> by dry method at 97 °C for 6 h to obtain optimum parameters for imparting a maximum bleaching power towards soybean oil. The H<sub>2</sub>SO<sub>4</sub> content in dry bentonite-acid mixture was changed between 0% and 70%. The natural and activated samples were examined by X-ray diffraction (XRD), N<sub>2</sub> adsorption–desorption, and *n*-butylamine adsorption (from the solution in cyclohexane). The specific surface area (*S*), specific micro–mesopore volume (*V*), mesopore size distribution (PSD), and surface acidity (*n<sub>m</sub>*) of the samples were determined. The bleaching power (BP) of each sample for alkali-refined soybean oil was determined. The *S*, *V*, *n<sub>m</sub>*, and BP increase after activation at various acid contents up to 40% H<sub>2</sub>SO<sub>4</sub> without any considerable change in crystal structure of the smectite. The BP is controlled more by the PSD rather than other adsorptive properties of the bleaching earth. The optimum parameters for activation to obtain maximum bleaching power, are H<sub>2</sub>SO<sub>4</sub>% = 50–60, *S* = 250–230 m<sup>2</sup> g<sup>-1</sup>, *V* = 0.46–0.47 cm<sup>3</sup> g<sup>-1</sup>, *n<sub>m</sub>* = 9.0 × 10<sup>-4</sup>–8.4 × 10<sup>-4</sup> mol g<sup>-1</sup> and PSD mainly distributed between 1.4 and 6.0 nm.

© 2007 Elsevier Ltd. All rights reserved.

**Keywords:** Acid activation; Bentonite; Bleaching; Porosity; Surface acidity; Surface area

## 1. Introduction

Besides numerous industrial application areas, bentonites and their major clay mineral smectites have been used in food technology such as bleaching earth, clarification of beer and wine, animal feed bond, and food additives (Grim & Güven, 1978; Murray, 1991, 2000). Bentonites may also contain other clay- and non-clay minerals as impurities. Smectites generally are 2:1 layered, hydrated aluminum silicates. Bentonites are treated by the inorganic acids such as HNO<sub>3</sub>, HCl and H<sub>2</sub>SO<sub>4</sub> to remove some of the impurities and thereby to obtain more adsorptive materials (Heyding, Ironside, Norris, & Pryslazniuk, 1960; Komadel, 2003; Komadel et al., 1996; Komadel, Schmidt, Madejová, &

Čičel, 1990; Mills, Holmes, & Cornelius, 1950; Van Rompaey, Van Ranst, De Coninck, & Vindevogel, 2002). Due to their widespread use in edible oil bleaching, the activated bentonites are called as bleaching earths (Beneke & Lagaly, 2002; Boukerroui & Ouali, 2000; Christidis, Scott, & Dunham, 1997; Griffiths, 1990; Siddiqui, 1968; Tsai, Chang, Lai, & Lo, 2005).

Crude edible oils obtained by solvent extraction or compression from plants such as soybean, safflower, sunflower, corn, cottonseed, rapeseed, mustard seed, sesame, palm, peanut, coconut and olive, can be processed by chemical or physical refining techniques (Mounts, 1981). The conventional chemical technique consists of water or acid degumming, caustic refining, deodorization, and winterization steps. Besides color pigments, other impurities such as soap, sulphur, phosphates, trace metals, and oxidation products are removed from the alkali-refined oils by bleaching (Falaras, Kovanis, Lezou,

\* Corresponding author. Tel.: +90 312 2126720/1014; fax: +90 312 2232395.

E-mail address: [sakaya@science.ankara.edu.tr](mailto:sakaya@science.ankara.edu.tr) (Y. Sarıkaya).

& Seiragakis, 1999; Kheok & Lim, 1982; Morgan, Shaw, Sidebottom, Soon, & Taylor, 1985; Oboh & Aworh, 1988; Rossi, Gianazza, Alamprese, & Stanga, 2003; Temuujin et al., 2006; Zschau, 2001). Bleaching is based on the physical adsorption, chemical adsorption, ion exchange, and chemical decomposition of coloring organic pigments and other impurities on the bleaching earth.

Like other adsorptive solids, the pores of a bleaching earth may be micropores (width  $<2$  nm), mesopores (width 2–50 nm) and macropores (width  $>50$  nm) (Gregg & Sing, 1982). The radius of a pore, assumed to be cylindrical, can be taken as half the pore width. The total volume of pores in 1 g of solid is defined as the specific pore volume ( $V$ ). The area of the inner and outer walls of the pores located intra- and interparticles in 1 g solid is taken as the specific surface area ( $S$ ). The adsorptive surface originates from the micro- and mesopores. The contribution of macropores on the surface area is negligible. Furthermore, bleaching earths behave as solid acids. Brønsted and Lewis acid sites on their surfaces are proton donors and electron pair acceptors, respectively (Brown & Rhodes, 1997a; Frenkel, 1974; Kumar, Jasra, & Bhat, 1995; Noyan, Önal, & Sarıkaya, 2006; Walling, 1950). The molar number of acid sites in 1 g solid is defined as surface acidity ( $n_m$ ). The acid strength of a surface can be characterized by the equilibrium constant ( $K$ ) of its neutralization reaction with a weak base such as ammonia, and amines (Benesi, 1956, 1957; Brown & Rhodes, 1997b; Loeppert, Zelazny, & Volk, 1986).

Bleaching power is dependent on the surface area, surface acidity, catalytic activity, porosity and pore size distribution of the bleaching earth (Boki, Kubo, Wada, & Tamura, 1992; Boki, Kubo, Kawasaki, & Mori, 1992; Breen, Zahoor, Madejová, & Komadel, 1997; González-Paradas, Villafranca-Sánchez, & Gallego-Campo, 1993; Önal, submitted for publication; Önal, Sarıkaya, Alemdaroğlu, & Bozdoğan, 2002; Srasra, Bergaya, Van Damme, & Ariguib, 1989; Vicente-Rodriguez, Suarez, Lopez-González, & Bánares-Munoz, 1996). These physicochemical properties of bleaching earths change depending on the mineralogical and chemical composition of the activated bentonite, type and concentration of the inorganic acid, used in the process and also temperature and time of activation.

The bleaching power of an acid-activated bentonite is generally examined on the basis of the  $\beta$ -carotene and chlorophyll adsorption capacities (González-Paradas, Villafranca-Sánchez, Socias-Viciano, & Gallego-Campo, 1994; Khoo, Morsingh, & Liew, 1979; Liew, Tan, Morsingh, & Khoo, 1982; Mokaya, Jones, Davies, & Whittle, 1993; Sarier & Güler, 1988, 1989). The adsorption mechanism has been discussed by using both the Langmuir and Freundlich isotherms (Sabah, Çınar, & Çelik, 2007; Topallar, 1998; Tsai, Chang, Ing, & Chang, 2004; Teng & Lin, 2006). The kinetics of the bleaching process has been examined on the basis of a first order reaction model applied to

chemical reactions (Brimberg, 1982; Christidis & Kosiari, 2003).

Although several workers mentioned above have made extensive studies on the numerous properties of bleaching earths and bleaching processes, no report specifically concentrated on the surface properties of bleaching earths has yet appeared. The aim of this study is to examine of the bleaching power of some  $H_2SO_4$ -treated bentonite samples by making use of surface area, surface acidity, porosity and mesopore size distribution parameters.

## 2. Materials and methods

### 2.1. Materials

A calcium-rich bentonite (CaB) sample from the Hançılı bed (Keskin, Ankara, Turkey) was used in the experiments. The effects of heating and acid activation on some physicochemical properties of this material were previously investigated (Noyan, Önal, & Sarıkaya, *in press*, submitted for publication). The bulk chemical analysis of the bentonite (mass %) is  $SiO_2$ , 60.85;  $TiO_2$ , 0.85;  $Al_2O_3$ , 16.50;  $Fe_2O_3$ , 5.74;  $MgO$ , 2.71;  $CaO$ , 2.37;  $Na_2O$ , 1.53;  $K_2O$ , 0.83 and loss on ignition (LOI), 8.40. The  $H_2SO_4$  (98%,  $d = 1.98$  g  $cm^{-3}$ ) and other chemicals used are of analytical grade and were supplied from Merck Chemical Company. The bentonite was ground to pass through a 0.074 mm (200 mesh) sieve, dried at 105 °C for 24 h, and stored in tightly closed plastic bottles for use in the experiments. Alkali-refined soybean oil used in the bleaching experiments was supplied from a vegetable oil plant (Marsa, İstanbul, Turkey).

### 2.2. Acid activation

Eleven samples, each having a mass of 40 g, were weighed from the dried bentonite powder. The samples were activated with  $H_2SO_4$  by dry method (Heyding et al., 1960). The content of  $H_2SO_4$  in dry bentonite-acid mixture was changed between 0% and 70% by mass. Acid content was increased in smaller increments around 40%  $H_2SO_4$ , the likely optimum rate by experience. Eleven gel-like mixtures were prepared by adding the concentrated acid having calculated amounts of  $H_2SO_4$ . Acid activation was conducted by heating the mixtures in an oven at 97 °C for 6 h. Each activated sample was suspended in water, and centrifuged. Obtained precipitate was washed with distilled water until it was free from  $SO_4^{2-}$  against 5%  $BaCl_2$  solution. After drying at 105 °C for 4 h, the activated samples were stored in tightly closed plastic bottles. In this way, eleven bleaching earths were obtained. Prior experience (Noyan et al., 2006; Önal et al., 2002; Önal & Sarıkaya, 2007) with same and other bentonites indicates that the physicochemical properties of acid treated bentonite samples do not differ appreciably from batch to batch. Therefore, acid treatment procedures were done once.

### 2.3. Instrumentation

The X-ray diffraction (XRD) patterns of natural and acid activated samples were recorded from random mounts prepared by glass slide method using a Rigaku D-Max 2200 Powder Diffractometer, operating at 40 kV and 30 mA, using Ni-filtered  $\text{CuK}\alpha$  radiation having 0.15418 nm wavelength, at a scanning speed of  $2^\circ 2\theta \text{ min}^{-1}$  (Moore & Reynolds, 1997).

The adsorption and desorption isotherms of  $\text{N}_2$ , at liquid  $\text{N}_2$  temperature, on the natural and acid activated samples were determined by a volumetric adsorption instrument of pyrex glass connected to a high vacuum system (Sarıkaya & Aybar, 1978; Sarıkaya, Önal, Baran, & Alemdaroğlu, 2000; Sarıkaya, Sevinç, & Akinç, 2001). Before measurements, the samples were outgassed at  $150^\circ\text{C}$  for 4 h under a vacuum of  $10^{-3}$  mm Hg. The technique of gas adsorption manometry was used for the determination of the adsorbed amount (Rouquerol, Rouquerol, & Sing, 1999; Sing, 2001). This point-by-point procedure is based on the measurement of the gas pressure in a calibrated constant volume at a known temperature. Pre-calibrated dosing volume at dead space volume on the adsorbent bulb was kept constant by the pressure measurements with mercury manometers. Pressure of dosing chamber was measured at room temperature before and after nitrogen allowed to enter adsorbent bulb. Dead space pressure, which is also equilibrium pressure of adsorption, was measured for each point. The amount adsorbed was calculated for each point by evaluating the known parameters. For each point, the cumulative amount of the adsorbed nitrogen until equilibrium pressure was reached, has been taken as the attained adsorption capacity.

The adsorption of *n*-butylamine, from a cyclohexane-solution, on the natural and acid-activated samples was recorded by a UV-VIS spectrophotometer (Varian, Cary 50). In each experiment, a series of 10 mL test tubes was loaded with 0.1 g of bentonite sample. Then, to each tube, 10 mL of freshly prepared *n*-butylamine solutions (in cyclohexane) with a concentration ranging from  $2.0 \times 10^{-3}$  M to  $1.8 \times 10^{-2}$  M were pipetted. To reach adsorption equilibrium, the tubes were shaken mechanically at  $25^\circ\text{C}$  for 75 h. The absorbance values of the solutions were then measured at the wavelength of maximum absorption,  $\lambda = 227$  nm, and equilibrium concentrations were determined from a calibration plot.

Each bleaching experiment was carried out in an open 400 mL beaker containing a stirred suspension of a 1% by mass bleaching earth in alkali-refined soybean oil. The mixture was then heated to  $95\text{--}105^\circ\text{C}$ , kept at this temperature interval for 15 min, similar to the standard AOCS procedures (Chamkasem & Johnson, 1988; Önal, submitted for publication). The oil was then filtered through Whatman No. 41 filter paper. The color index of the oil, in red-yellow units, was determined by using a Lovibond Automatic Tintometer (Type D) equipped with 2.54 cm cells according to the AOCS Official Method Cc 13b-45 (1973).

## 3. Result and discussion

### 3.1. XRD analysis

The XRD powder-patterns for some representative bentonites, natural and acid-activated, are given in Fig. 1. The bentonite investigated displays peaks belonging to the clay mineral smectite (with a  $d_{001}$  value of 1.49 nm), and non-clay minerals, quartz, opal, and feldspar. Characteristic XRD peaks were identified according to the literature (Moore & Reynolds, 1997). The XRD patterns show that the crystallinity of the smectite decreases when the mass-percentage of  $\text{H}_2\text{SO}_4$  in the acid treatment exceeds 10%. However, the crystal structure of the smectite is still partly preserved even after activation with a  $\text{H}_2\text{SO}_4$  content of 50% by mass. The crystallinity of the non-clay minerals are not affected by the acid activation process.

### 3.2. Nitrogen adsorption and desorption isotherms

The  $\text{N}_2$  adsorption/desorption isotherms at the liquid  $\text{N}_2$  temperature ( $\sim 77$  K) for natural and all acid-activated samples were examined, and representative ones, for natural and acid-activated samples are shown in Fig. 2. Here,  $p$  is the adsorption and desorption equilibrium pressure,  $p^0$  is the vapor pressure of bulk liquid nitrogen at experimental temperature,  $p/p^0 = x$  is the relative equilibrium pressure, and  $n$  is the adsorption capacity defined as the number of moles of nitrogen adsorbed on 1 g of sample at any  $x$ .

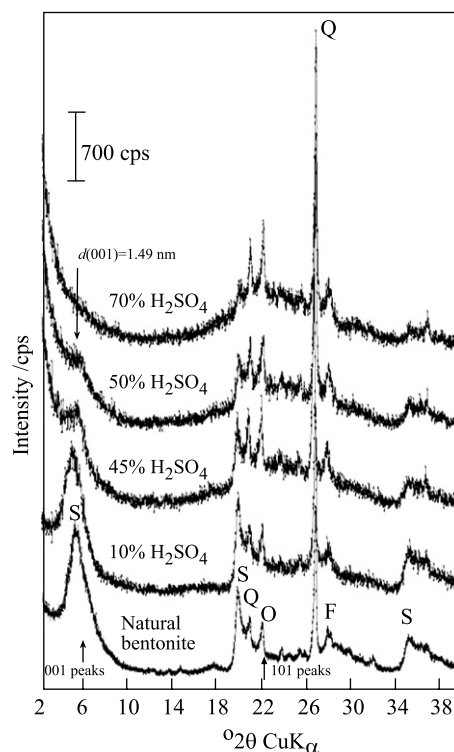


Fig. 1. XRD patterns of natural bentonite and some acid activated samples (S: smectite, Q: quartz, O: opal, F: feldspar).

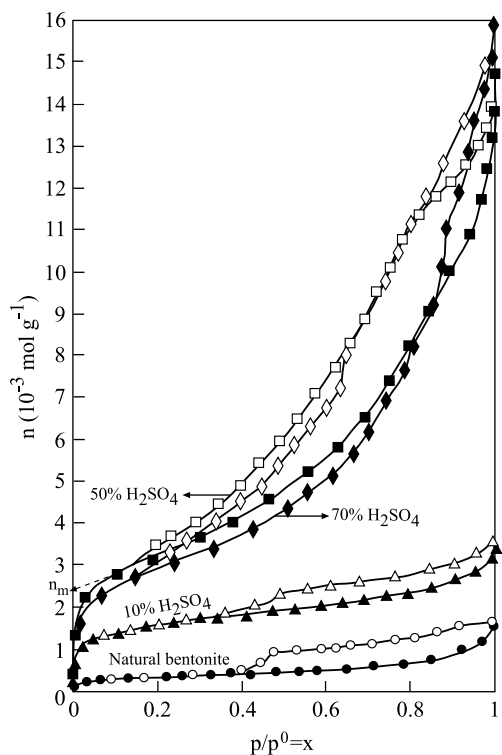


Fig. 2. Adsorption/desorption isotherms of  $N_2$  at liquid  $N_2$  temperature for natural bentonite and some acid activated samples.

The isotherms show that the adsorption capacity increases with increasing acid content up to 50%  $H_2SO_4$  and then decreases slowly through 70%  $H_2SO_4$ .

According to Brunauer, the classification of these isotherms is similar to Type II (Brunauer, Deming, Deming, & Teller, 1940). The shapes of the adsorption/desorption isotherms indicate that the prepared bleaching earths are mainly mesoporous solids but also contain some micropores. The overlapping of the adsorption/desorption isotherms over the interval  $0.35 < x < 0.96$  shows that the multimolecular and monomolecular adsorptions are reversible. After multimolecular adsorption was complete at  $x = 0.35$ , capillary condensation begins, and all mesopores filled up to  $x = 0.96$ . Bulk liquid nitrogen forms at  $x = 1$  (Linsen, 1970). At the interval of  $1 < x < 0.96$ , the liquid nitrogen outside the mesopores evaporates spontaneously so long as the relative equilibrium pressure due to desorption is low enough. The same is true for the liquid nitrogen within the mesopores at the interval,  $0.96 < x < 0.35$ . The shapes of mesopores in a solid may be of cylindrical-, parallel-sides-, slit-, and wedge-shaped or like an ink-bottle. Capillary condensation begins in the narrowest mesopores first, while capillary evaporation starts earlier in the largest mesopores. This difference is the major cause of the hysteresis between adsorption and desorption isotherms. The hysteresis phenomenon becomes more prominent with acid activation because the amount of mesopores increases by the structural deformation. Due to the same reason, capillary condensation on acid-

treated (50–70%  $H_2SO_4$ ) bentonite is discernible under a relative pressure of  $x \cong 0.2$  while, with the natural material, capillary condensation can only occur at  $x = 0.4$ .

### 3.3. Surface area

The specific surface areas of the samples were obtained from the standard Brunauer, Emmett and Teller (BET) method by using the adsorption data of  $N_2$  in the interval  $0.05 < x < 0.35$  (Brunauer, Emmett, & Teller, 1938; Everett, Parfitt, Sing, & Wilson, 1974; McClellan & Hornsberger, 1967; Sarıkaya, Ada, Alemdaroğlu, & Bozdoğan, 2002). The representative BET plots were given in Fig. 3. These plots fit to the BET equation in the form

$$x/n(1-x) = 1/n_m x + [(c-1)/n_m c]x \quad (1)$$

where,  $n_m$  is the monomolecular adsorption capacity and  $c$  is a constant. The values  $n_m$  and  $c$  were determined by solving the simultaneous equations obtained from the slope and intercept of the BET straight line. The specific surface areas,  $S/m^2 g^{-1}$ , were calculated from the equation

$$S = n_m N_A a_m \quad (2)$$

where,  $N_A = 6.02 \times 10^{-23} \text{ mol}^{-1}$  is the Avogadro constant and  $a_m = 16.2 \times 10^{-20} \text{ m}^2$  is the area occupied by a single nitrogen molecule.

As seen in Fig. 3, the slope of BET straight lines decreases up to 50%  $H_2SO_4$  and then tends to increase slightly up to 70%  $H_2SO_4$ . A reverse behavior is also reflected in the surface area versus acid content plots (Fig. 4). As seen in Fig. 4, the  $S$  value increases rapidly from  $25 \text{ m}^2 g^{-1}$  to its maximum value of  $285 \text{ m}^2 g^{-1}$  as the acid content increases from zero to 40–45%  $H_2SO_4$ , and then decreases slowly.

### 3.4. Micro-mesopore volume

All micro- and mesopores are full with liquid nitrogen by desorption at  $x = 0.96$ , as mentioned above. Hence,

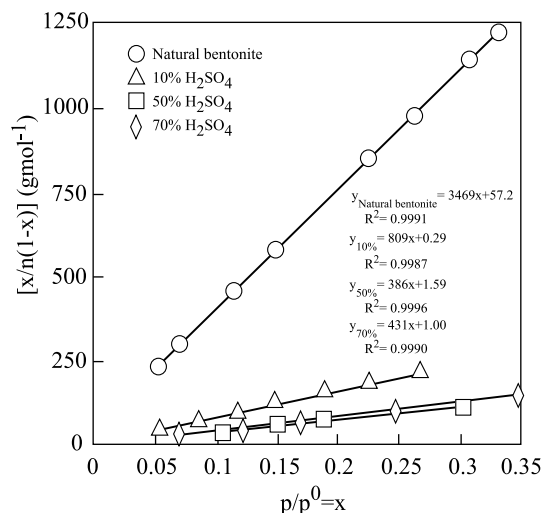


Fig. 3. BET plots for natural bentonite and some acid activated samples.



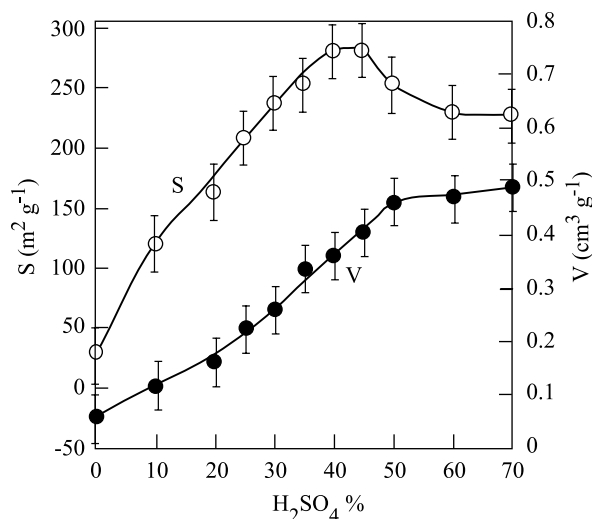


Fig. 4. Variation of the specific surface area ( $S$ ) and the specific micro-mesopore volume ( $V$ ) with the  $H_2SO_4$  content in activation.

the adsorption capacities as liquid nitrogen volumes estimated from desorption isotherms at  $x = 0.96$  are taken as the specific micro-mesopore volumes,  $V/\text{cm}^3 \text{g}^{-1}$ , of the samples.

The variation of the micro-mesopore volume with the  $H_2SO_4$  content used in activation is shown in Fig. 4. The  $V$  value increases rapidly from  $0.05 \text{ cm}^3 \text{g}^{-1}$  to  $0.45 \text{ cm}^3 \text{g}^{-1}$  as the acid content changes from zero to 50%  $H_2SO_4$ , and then stays approximately constant. The  $S$  and  $V$  curves do not change parallel as seen in Fig. 4. The increase in porosity is due to the partial dissolution of the exchangeable cations such as  $\text{Na}^+$  and  $\text{Ca}^{2+}$ , and also structural cations such as  $\text{Al}^{3+}$ ,  $\text{Fe}^{3+}$ , and  $\text{Mg}^{2+}$  from 2:1 layers of the smectite mineral.

### 3.5. Pore size distribution

The pore size distributions (PSD) of the samples were obtained and representative curves are given in Fig. 5. Here,  $r$  is the radius of the mesopores (assumed to be cylindrical) and  $V$  is the specific micro-mesopore volume. The  $r$  values were calculated from desorption isotherms by using corrected Kelvin equation which is a relationship between  $r$  and  $x$  values (Gregg & Sing, 1982; Önal & Sarıkaya, 2007). The  $V$  values corresponding to  $r$  values were also calculated from the desorption isotherms as the liquid nitrogen volumes for each  $x$ . The area under the PSD curve and two known abscissa values is related to the relative amount of mesopores having sizes that fall into the range defined by the abscissa limits. The most abundant approximate pore size increases from 1.84 to 2 nm up to 50%  $H_2SO_4$ , probably due to the transformation of some micropores to mesopores during the development of the activation. Seventy percent of  $H_2SO_4$  sample has two maxima at 1.84 and 2.68 nm. On the other hand, the area of the PSD curve increases with increasing acid content as seen in Fig. 5. After the 50% acid content, all samples have maximum  $r$

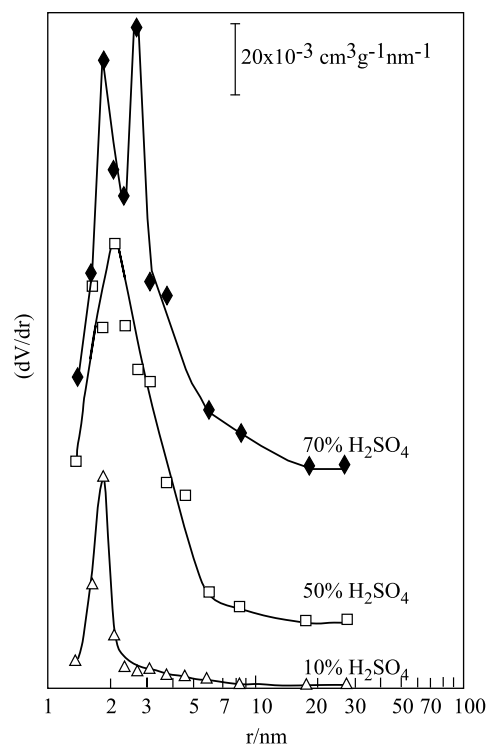


Fig. 5. Mesopore size distribution (PSD) curves of some acid activated samples.

values and the area of PSD curves display a slight increase. This indicates that the rate of transformation of micropores to mesopores decreases. So the rapid increases in the  $S$  and  $V$  values decreases by the activation above the 50%  $H_2SO_4$  as seen in Fig. 4.

### 3.6. Surface acidity

The average surface acidity ( $n_m/\text{mol g}^{-1}$ ) of each sample was determined from three Langmuir plots drawn by using the data obtained from  $n$ -butylamine adsorptions (Brown & Rhodes, 1997a; Noyan et al., 2006; Varma, 2002). The surface acidity versus the  $H_2SO_4$  content is shown in Fig. 6. The  $n_m$  value increases rapidly from  $4.2 \times 10^{-4}$  to  $9.4 \times 10^{-4} \text{ mol g}^{-1}$  with an increase of the acid content from zero to 45%  $H_2SO_4$ . The result shows that the surface acidity and surface area change parallel to each other by the activation.

### 3.7. Bleaching power

Bleaching or decolorizing power (BP) of the bleaching earths was calculated from the equation;

$$\text{BP} = 100(R_0 - R)/R_0 \quad (3)$$

where,  $R_0$  and  $R$  are the red color units on Lovibond scale of the alkali-refined oil before and after bleaching. The variation of the BP with the  $H_2SO_4$  content is seen in Fig. 6. The BP value increases rapidly from 3 to 70 with an increase of the acid content from zero to 50–60%  $H_2SO_4$ ,

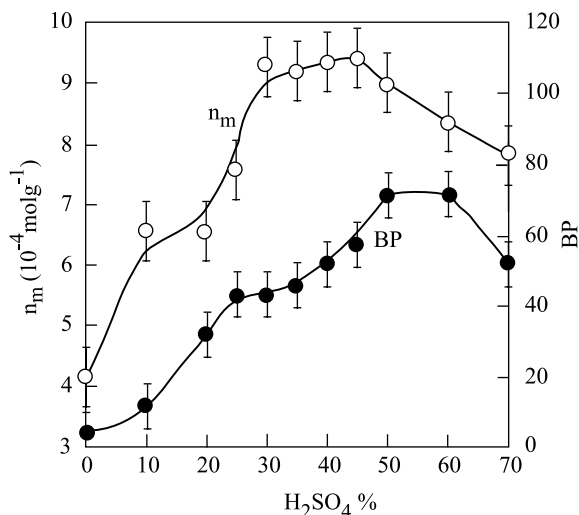


Fig. 6. Variation of the surface acidity ( $n_m$ ) and the bleaching power (BP) by increasing  $H_2SO_4$  content in activation.

and then decreases slowly. Although the changes in the  $S$ ,  $V$ ,  $n_m$ , and BP are similar until up to the 40%  $H_2SO_4$ , their maxima do not exactly overlap. However, the BP does not have a maximum when  $S$ ,  $V$ , and  $n_m$  reach to their maxima. The BP reaches to a maximum at the optimum conditions, i.e., 50–60%  $H_2SO_4$ ,  $S = 250\text{--}230\text{ m}^2\text{ g}^{-1}$ ,  $V = 0.46\text{--}0.47\text{ cm}^3\text{ g}^{-1}$ , and  $n_m = 9.0 \times 10^{-4}\text{--}8.4 \times 10^{-4}\text{ mol g}^{-1}$ . The maximum BPs of this bleaching earth and commercial Tonsil 131 (Süd Chemie) are comparable as 0.71 and 0.69, respectively. This shows that bleaching earth prepared under optimum conditions is suitable for industrial uses. With an acid content of 50%, the area of the PSD curve reaches a maximum value and  $r$  is fit to the sizes of pigments as seen in Fig. 5. The large-size, colored organic pigments in the soybean oil can penetrate into the mesopores with a radius between 1.4 and 3.0 nm and strongly adsorbed on their surface. However, the BP is mainly controlled by the PSD, rather than the other adsorptive properties.

As to oil retention characteristics of the natural and acid-activated bentonites, the natural material is found to have trapped some mass of oil roughly 20% of its own weight after use, whereas, after acid-activation, the relative mass of oil increases up to 40%. In summary, oil retainment property increases as the acid content in activation increases, but never exceeds 40%.

#### 4. Conclusion

The exchangeable, and to a lesser extent, structural cations of the smectite in a bentonite are removed by acid activation. The surface area, micro-mesopore volume, mesopore size distribution, surface acidity and bleaching power of a bentonite are greatly affected from acid activation at limited acid contents without any considerable change in crystal structure of the smectite. Although, the bleaching power increases with increasing surface area,

porosity and surface acidity, it depends more on the mesopore size distribution of the bleaching earth. The bleaching earths obtained by acid activation are more porous materials than the natural bentonite for use as adsorbents, filtering medium, catalyst and precursors for pillared clays.

#### Acknowledgements

The authors thank the Scientific Research Council of Ankara University, Turkey for supporting this study under a Project No: 2003.07.05.082.

#### References

- AOCS (1973). Official method Cc 13b-45 color determination by tintometer. *Journal of the American Chemical Society*.
- Beneke, K., & Lagaly, G. (2002). From fuller's earth to bleaching earth: A historical note. *ECGA (European Clay Group Association) Newsletter*, 5, 57–78.
- Benesi, H. A. (1956). Acidity of catalyst surfaces. I. Acid strength from colors of adsorbed indicators. *The Journal of the American Chemical Society*, 78, 5490–5494.
- Benesi, H. A. (1957). Acidity of catalyst surfaces. II. Amine titration using Hammett indicators. *The Journal of Physical Chemistry*, 61, 970–973.
- Boki, K., Kubo, M., Kawasaki, N., & Mori, H. (1992). Adsorption isotherms of pigments from alkali-refined vegetable oils with clay minerals. *Journal of the American Oil Chemists Society*, 69, 372–378.
- Boki, K., Kubo, M., Wada, T., & Tamura, T. (1992). Bleaching of alkali-refined vegetable oils with clay minerals. *Journal of the American Oil Chemists Society*, 69, 233–236.
- Boukerroui, A., & Ouali, M. S. (2000). Regeneration of a spent bleaching earth and its reuse in the refining of an edible oil. *Journal of Chemical Technology and Biotechnology*, 75, 773–776.
- Breen, C., Zahoor, E. D., Madejová, J., & Komadel, P. (1997). Characterization and catalytic activity of acid-treated size-fractionated smectites. *The Journal of Physical Chemistry B*, 101, 5324–5331.
- Brimberg, U. I. (1982). Kinetics of bleaching of vegetable oils. *Journal of the American Oil Chemists Society*, 59, 74–78.
- Brown, D. R., & Rhodes, C. N. (1997a). Bronsted and Lewis acid catalysis with ion-exchanges clays. *Catalysis Letters*, 45, 35–40.
- Brown, D. R., & Rhodes, C. N. (1997b). A new technique for measuring surface acidity by ammonia adsorption. *Thermochimica Acta*, 294, 33–37.
- Brunauer, S., Deming, L. S., Deming, D. M., & Teller, E. (1940). On a theory of the van der Waals adsorption on gases. *Journal of the American Chemical Society*, 62, 1723–1732.
- Brunauer, S., Emmett, P. H., & Teller, E. (1938). Adsorption of gases in multimolecular layers. *Journal of the American Chemical Society*, 60, 308–319.
- Chamkasem, N., & Johnson, L. A. (1988). Color stability of glandless cottonseed oil. *Journal of the American Oil Chemists Society*, 65, 1778–1780.
- Christidis, G. E., & Kosiari, S. (2003). Decolorization of vegetable oils: a study of the mechanism of adsorption of  $\beta$ -carotene by an acid-activated bentonite from Cyprus. *Clays and Clay Minerals*, 51, 327–332.
- Christidis, G. E., Scott, P. W., & Dunham, A. C. (1997). Acid activation and bleaching capacity of bentonites from the island of Milos and Chios, Aegean, Greece. *Applied Clay Science*, 12, 329–347.
- Everett, D. H., Parfitt, G. D., Sing, K. S. W., & Wilson, R. (1974). The SCI/IUPAC/NPL project on surface area standards. *Journal of Applied Chemistry and Biotechnology*, 24, 199–219.
- Falaras, P., Kovanis, I., Lezou, F., & Seiragakis, G. (1999). Cottonseed oil bleaching by acid-activated montmorillonite. *Clay Minerals*, 34, 221–232.

- Frenkel, M. (1974). Surface acidity of montmorillonites. *Clays and Clay Minerals*, 22, 435–441.
- González-Paradas, E., Villafranca-Sánchez, M., & Gallego-Campo, A. (1993). Influence of the physical–chemistry properties of an acid activated bentonite in the bleaching of olive oil. *Journal of Chemical Technology and Biotechnology*, 57, 213–216.
- González-Paradas, E., Villafranca-Sánchez, M., Socias-Viciano, M., & Gallego-Campo, A. (1994). Adsorption chlorophyll from acetone solution on natural and activated bentonite. *Journal of Chemical Technology and Biotechnology*, 61, 175–178.
- Gregg, S. J., & Sing, K. S. W. (1982). *Adsorption, surface area and porosity* (2nd ed.). London: Academic Press.
- Griffiths, J. (1990). Acid activated bleaching clays. *Industrial Minerals*, 276, 55–67.
- Grim, R. E., & Güven, N. (1978). *Bentonites – geology, mineralogy, properties and uses. Developments in Sedimentology* (Vol. 24). New York: Elsevier.
- Heyding, R. D., Ironside, R., Norris, A. R., & Prysazniuk, R. Y. (1960). Acid activation of montmorillonite. *Canadian Journal of Chemistry*, 38, 1003–1016.
- Kheok, S. C., & Lim, E. E. (1982). Mechanism of palm oil bleaching by montmorillonite clay activated at various acid concentrations. *Journal of the American Oil Chemists Society*, 59, 129–131.
- Khoo, L. E., Morsingh, F., & Liew, K. Y. (1979). The adsorption of  $\beta$ -carotene. I. By bleaching earths. *Journal of the American Oil Chemists Society*, 59, 672–675.
- Komadel, P. (2003). Chemically modified smectites. *Clay Minerals*, 38(11), 127–138.
- Komadel, P., Madejová, J., Janek, M., Gates, W. P., Kirkpatrick, R. J., & Stucki, J. W. (1996). Dissolution of hectorite in inorganic acids. *Clays and Clay Minerals*, 44(2), 228–236.
- Komadel, P., Schmidt, D., Madejová, J., & Čičel, B. (1990). Alteration of smectites by treatments with hydrochloric acid and sodium carbonate solutions. *Applied Clay Science*, 5, 113–122.
- Kumar, P., Jasra, R. V., & Bhat, T. S. G. (1995). Evolution of porosity and surface acidity in montmorillonite clay on acid activation. *Industrial and Engineering Chemistry Research*, 34, 1440–1448.
- Liew, K. Y., Tan, S. H., Morsingh, F., & Khoo, L. E. (1982). Adsorption of  $\beta$ -carotene: II. On cation exchanged bleaching clays. *Journal of the American Oil Chemists Society*, 59, 480–484.
- Linsen, B. G. (1970). *Physical and chemical aspects of adsorbents and catalysts*. London: Academic Press.
- Loeppert, R. H., Zelazny, L. W., & Volk, B. G. (1986). Acidic properties of montmorillonite in selected solvents. *Clays and Clay Minerals*, 34, 87–92.
- McClellan, A. L., & Hornsberger, H. F. (1967). Cross-sectional areas of molecules adsorbed on solid surfaces. *Journal of Colloid and Interface Science*, 23, 577–599.
- Mills, G. A., Holmes, J., & Cornelius, E. B. (1950). Acid activation of some bentonite clays. *Journal of Physics and Colloid Chemistry*, 54, 1170–1185.
- Mokaya, R., Jones, W., Davies, M. E., & Whittle, M. E. (1993). Chlorophyll adsorption by alumina-pillared acid activated clays. *Journal of the American Oil Chemists Society*, 70, 241–244.
- Moore, D. M., & Reynolds, R. C. Jr., (1997). *X-ray diffraction identification and analysis of clay minerals* (2nd ed.). Oxford: Oxford University Press.
- Morgan, D. A., Shaw, D. B., Sidebottom, T. C., Soon, T. C., & Taylor, R. S. (1985). The function of bleaching earths in the processing of palm kernel and coconut oils. *Journal of the American Oil Chemists Society*, 62, 292–299.
- Mounts, T. L. (1981). Chemical and physical effects of processing fats and oils. *Journal of the American Oil Chemists Society*, 58, 51A–54A.
- Murray, H. H. (1991). Overview – clay mineral applications. *Applied Clay Science*, 5, 379–395.
- Murray, H. H. (2000). Traditional and new applications for kaolin, smectite and palygorskite: A general overview. *Applied Clay Science*, 17, 207–221.
- Noyan, H., Önal, M., & Sarıkaya, Y. (2006). The effect of heating on the surface area, porosity and surface acidity of a bentonite. *Clays and Clay Minerals*, 54, 375–381.
- Noyan, H., Önal, M., & Sarıkaya, Y. (in press). Thermal deformation thermodynamics of a smectite mineral. *Journal of Thermal Analysis and Calorimetry*.
- Noyan, H., Önal, M., & Sarıkaya, Y. (submitted for publication). Acid activation thermodynamics of a bentonite. *Clays and Clay Minerals*.
- Oboh, A. O., & Aworh, O. C. (1988). Laboratory trials on bleaching palm oil with selected acid-activated Nigerian clays. *Food Chemistry*, 27, 311–317.
- Önal, M. (submitted for publication). Changes in bleaching power of acid activated bentonite samples for soybean and cottonseed oils. *Journal of the American Oil Chemists Society*.
- Önal, M., & Sarıkaya, Y. (2007). Preparation and characterization of acid activated bentonite powder. *Powder Technology*, 172, 14–18.
- Önal, M., Sarıkaya, Y., Alemdaroğlu, T., & Bozdoğan, I. (2002). The effect of acid activation on some of the physicochemical properties of a bentonite. *Turkish Journal of Chemistry*, 26, 409–416.
- Rossi, M., Gianazza, M., Alamprese, C., & Stanga, F. (2003). The role of bleaching clays and synthetic silica in palm oil physical refining. *Food Chemistry*, 82, 291–296.
- Rouquerol, F., Rouquerol, J., & Sing, K. (1999). *Adsorption by powder and porous solids*. London: Academic Press.
- Sabah, E., Çınar, M., & Çelik, M. S. (2007). Decolorization of vegetable oils: Adsorption mechanism of  $\beta$ -carotene on acid-activated sepiolite. *Food Chemistry*, 100, 1661–1668.
- Sarıer, N., & Güler, G. (1988).  $\beta$ -Carotene adsorption on activated montmorillonite. *Journal of the American Oil Chemists Society*, 65, 776–779.
- Sarıer, N., & Güler, G. (1989). The mechanism of  $\beta$ -carotene adsorption on activated montmorillonite. *Journal of the American Oil Chemists Society*, 66, 917–923.
- Sarıkaya, Y., Ada, K., Alemdaroğlu, T., & Bozdoğan, I. (2002). The effect of  $Al^{3+}$  concentration on the properties of alumina powders obtained by reaction between aluminum sulphate and urea in boiling aqueous solution. *Journal of the European Ceramic Society*, 22, 1905–1910.
- Sarıkaya, Y., & Aybar, S. (1978). The adsorption of  $NH_3$ ,  $N_2O$  and  $CO_2$  gases on the 5A molecular sieve. *Communication Faculty of Science University of Ankara*, B24, 33–39.
- Sarıkaya, Y., Önal, M., Baran, B., & Alemdaroğlu, T. (2000). The effect of thermal treatment on some of the physicochemical properties of a bentonite. *Clays and Clay Minerals*, 48, 557–562.
- Sarıkaya, Y., Sevinç, I., & Akınç, M. (2001). The effect of calcination temperature on some of the adsorptive properties of fine alumina powders produced by emulsion evaporation. *Powder Technology*, 116, 109–114.
- Siddiqui, M. K. H. (1968). *Bleaching Earths*. Oxford: Pergamon.
- Sing, K. (2001). The use of nitrogen adsorption for characterization of porous materials. *Colloid and Surfaces A: Physicochemical and Engineering Aspects*, 187–188, 3–9.
- Srasra, E., Bergaya, F., Van Damme, H., & Ariguib, N. K. (1989). Surface properties of an activated bentonite-decolourization of rape-seed oil. *Applied Clay Science*, 4, 411–421.
- Temuujin, J., Senna, M., Jadamba, T., Burmaa, D., Erdenechimeg, S., & MacKenzie, K. J. D. (2006). Characterization and bleaching properties of acid-leached montmorillonite. *Journal of Chemical Technology and Biotechnology*, 81, 688–693.
- Teng, M. Y., & Lin, S. H. (2006). Removal of basic dye from water onto pristine and HCl-activated montmorillonite in fixed beds. *Desalination*, 194, 156–165.
- Topallar, H. (1998). The adsorption isotherms of the bleaching of sunflower-seed oil. *Turkish Journal of Chemistry*, 22, 143–148.
- Tsai, W. T., Chang, C. Y., Ing, C. H., & Chang, C. F. (2004). Adsorption of acid dyes from aqueous solution on activated bleaching earth. *Journal of Colloid and Interface Science*, 275, 72–78.

- Tsai, W. T., Chang, Y. M., Lai, C. W., & Lo, C. C. (2005). Adsorption of basic dyes in aqueous solution by clay adsorbent from regenerated bleaching earth. *Applied Clay Science*, 29, 149–154.
- Van Rompaey, K., Van Ranst, E., De Coninck, F., & Vindevogel, N. (2002). Dissolution characteristics of hectorite in inorganic acids. *Applied Clay Science*, 21(5–6), 241–256.
- Varma, R. S. (2002). Clay and clay-supported reagents in organic synthesis. *Tetrahedron*, 58(7), 1235–1255.
- Vicente-Rodriguez, M. A., Suarez, M., Lopez-González, J. D., & Bánares-Munoz, M. A. (1996). Characterization, surface area and porosity analyses of the solids obtained by acid leaching of a saponite. *Langmuir*, 12, 566–572.
- Walling, C. (1950). The acid strength of surface. *Journal of American Chemical Society*, 72, 1164–1168.
- Zschau, W. (2001). Bleaching of edible fats and oils. *European Journal of Lipid Science and Technology*, 103, 505–551.